Separation Science and Technology
Publication details, including instructions for authors and subscription information:
http://www.informaworld.com/smpp/title~content=t713708471

Correlation of Filtrate Flow Rate for Irradiated and Unirradiated Tetraphenylborate Slurries

R. A. Peterson[a]; C. A. Nash[a]; D. J. McCabe[a]
[a] Westinghouse Savannah River Company Savannah River Technical Center, Aiken, SC

To cite this Article Peterson, R. A. , Nash, C. A. and McCabe, D. J.(1997) 'Correlation of Filtrate Flow Rate for Irradiated and Unirradiated Tetraphenylborate Slurries', Separation Science and Technology, 32: 1, 721 — 736
To link to this Article: DOI: 10.1080/01496399708003226
URL: http://dx.doi.org/10.1080/01496399708003226

SEPARATION SCIENCE AND TECHNOLOGY, 32(1-4), pp. 721-736, 1997

CORRELATION OF FILTRATE FLOW RATE FOR IRRADIATED AND UNIRRADIATED TETRAPHENYLBORATE SLURRIES

R. A. Peterson
C. A. Nash
D. J. McCabe

Westinghouse Savannah River Company
Savannah River Technical Center
Aiken, SC 29808

ABSTRACT

The filtrate flow rates obtained during the cross-flow filtration of slurries are dependent on the properties of the slurry particles. Tetraphenylborate is used to precipitate radioactive cesium from supernate salt solutions at the Savannah River Site. These slurries are then processed by a sequence of filtration steps. However, prior to the last filtration step, the slurries are exposed to significant doses of irradiation that appear to dramatically change the properties of these particles. A concomitant decrease in filter performance has been observed. An empirical model has been developed to predict the impact of irradiation on filtration. This model also predicts the dependency of performance on axial velocity and pressure drop.

INTRODUCTION

A process has been developed at the Savannah River Site for stabilizing High-Level Waste via vitrification for long-term storage. The waste present in the storage tanks at SRS can be divided into two segments: salt cake and sludge. Components of both of these waste streams are fed to the same vitrification process. This paper will focus on the initial processing steps for the salt cake. This stream contains significant quantities of Cs-137, Sr-85, and actinides. The initial processing steps for the salt cake are outlined in Figure 1.

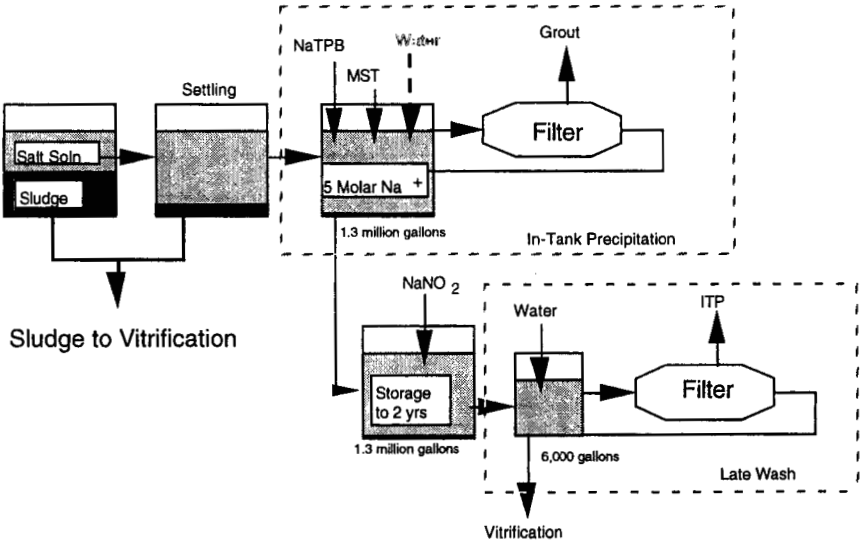

FIGURE 1. Salt solution processing scheme.

Once the salt cake has been dissolved and removed from the waste tank, most of the insoluble solids are removed by settling. The salt solution is then decanted to another tank where sodium tetraphenylborate (NaTPB) and monosodium titanate (MST) are added. The addition of NaTPB causes the precipitation of Cs-137. However, most of the TPB is consumed by the precipitation of KTPB. Strontium ion exchanges with MST, while actinides adsorb to the MST. The resultant solution is 5 M in Na+ with a very low concentration of free soluble radionuclides. To reduce the final volume of glass produced, this stream is concentrated by a factor of 10 via filtration. The filtrate is sent to a grout facility for immobilization as Low-Level Waste. The slurry is then washed to remove sodium via addition of water and removal of filtrate. This wash step is necessary to produce the required properties in the final glass form. The filtrate is again immobilized as grout.

This concentration and washing occur as a batch process. The product slurry may then be stored for a period expected to be up to 2 years prior to transfer to the vitrification process. However, to eliminate corrosion during storage, nitrite is added to the slurry. This nitrite must be removed via washing prior to transport of the slurry to the vitrification process. During storage, the slurry receives a large dose of irradiation (100

Mrad/year) from the entrained radionuclides. This exposure to irradiation changes the properties of the slurry particles. In particular, significant changes in slurry particle size and slurry viscosity are observed. The purpose of this paper is to explore the impact of these changes on filtration during the final washing step.

Construction of the facility to perform this final washing step has not yet reached completion. Prior to initiating radioactive operations with this facility, tests will be completed using a simulated waste stream. Due to cost and time limitations associated with irradiating a sufficient volume of simulant material, these tests will employ unirradiated simulants. The primary goal of this work is to develop a correlation of filter performance that can be employed to relate performance obtained during facility tests with unirradiated material to the expected performance with irradiated material. This correlation can be used to illuminate some of the limitations of existing theoretical models and indicate areas of future interest for fundamental studies.

EXPERIMENTAL

Bench-scale filtration experiments were performed using the Experimental Laboratory Filter (ELF) system. A sketch of the ELF appears in Figure 2. The ELF contains one filter tube mounted horizontally. For this study, the unit employed a stainless steel Mott filter measuring 18 inches in length with an internal diameter of 0.575 inches and 0.4-micron pores. A Wilden positive displacement pump provided slurry flow. The pump was supplied with process air at 90 psi. Slurry flow through the filter tube and the pressure supplied to the filter were controlled by adjusting the discharge metering valve and the recycle valve. These valves were adjusted simultaneously to achieve the target axial velocity and feed pressure. In all cases, shell-side pressure was found to be negligible.

The process vessel was charged with 10 L of 10 wt % KTPB slurry prior to each filtration experiment. The slurry contained 2.1 g/L of monosodium titanate (MST), and some slurries contained 6000 mg/L of insoluble sludge solids. The aqueous phase of the feed slurry was prepared by adding the salts in the concentrations listed in Table 1 to the required volume of water.

Six different experimental conditions were employed. These conditions are listed in Table 2. Each of these experiments was performed in duplicate. The two variables in these studies were irradiation dose and concentration of insoluble solids. Three irradiation doses were studied: 0 Mrad, 90 Mrad, and 230 Mrad. Two insoluble sludge solids concentrations were studied: 0 and 6000 mg/L.

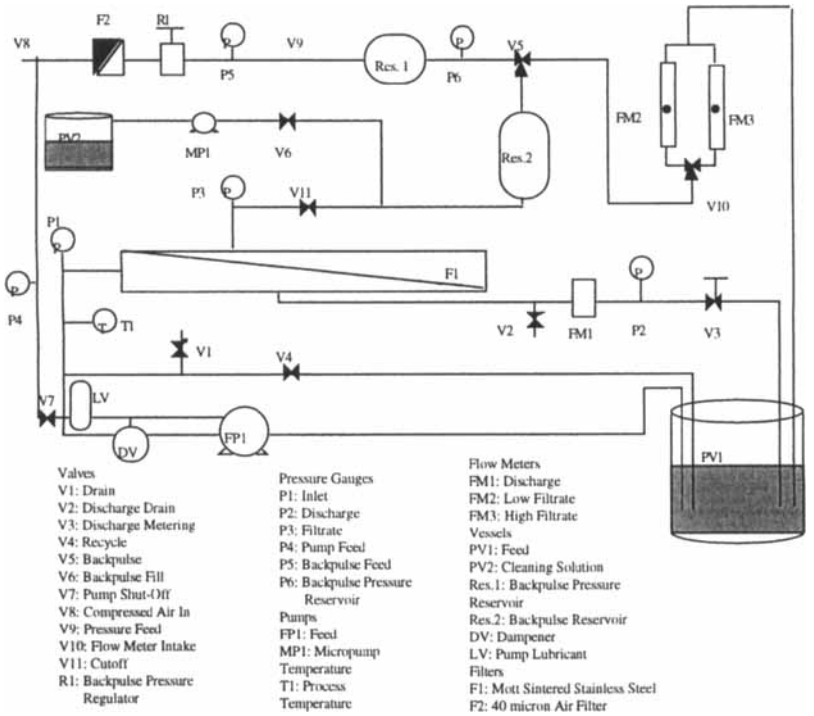

FIGURE 2. Experimental lab filter.

TABLE 1. INITIAL MATERIAL COMPOSITION

Component	Molarity
K_2CO_3	0.0017
KNO_2	0.23
KNO_3	0.04
Na_2SO_4	0.0015
NaTPB	0.27

TABLE 2. EXPERIMENTAL CONDITIONS

Experiment	Irradiation (Mrad)	Insolubles (mg/L)
1	0	0
2	0	6000
3	90	0
4	90	6000
5	230	0
6	230	6000

The irradiation was achieved using a cobalt-60 irradiation source. For those slurries that underwent irradiation, an additional precipitation was employed to capture potassium released during radiolytic decomposition. After irradiation, each sample was analyzed for soluble potassium. Then, sufficient excess sodium tetraphenylborate was added to precipitate the potassium and to bring the soluble tetraphenylborate ion concentration to 0.004 to 0.008 molar.

Purex sludge, a simulant developed at the Savannah River Site, was added to represent the sludge present in the slurry.[1] The composition of Purex sludge is listed in Table 3. The mean particle size, by volume, for this sludge was 12.6 microns (see Figure 3).[2] Note that sludge was not present during the irradiation of these slurries. Thus, the impact of sludge particles on the irradiation chemistry cannot be determined from these experiments.

Each experiment listed in Table 2 involved operating at 9 settings for the axial velocity and the feed pressure (one setting is repeated three times). The order of the test conditions is shown in Table 4 for each experiment. The axial velocity and pressure were set, and then a backpulse was performed at the start of each test. Process variables were measured every 10 minutes. (These variables included inlet, discharge and filtrate pressure, discharge flow rate, filtrate flow rate, and temperature.) Data were collected for a period of 30 minutes at which time a second backpulse was performed (4 data points per set of run conditions). At the conclusion of the second 30 minutes, the conditions were set for the next test and the above steps were repeated. The system temperature ranged between 21 and 28 °C.

For all sets of experimental conditions, the filtrate flux was averaged over the period between each backpulse. These filtrate flow rates were then

TABLE 3. SLUDGE COMPOSITION

Component	Wt % Solids (dry basis)
$Al(OH)_3$	17.9
$BaSO_4$	0.27
$Ca_3(PO_4)_2$	0.13
$CaCO_3$	4.54
$CaSO_4$	0.37
Cr_2O_3	0.27
$CsNO_3$	0.0066
CuO	0.13
$Fe(OH)_3$	42.1
HgO	1.28
KNO_3	0.017
KOH	0.33
MgO	0.25
MnO_2	6.36
Mn_3O_4	0.71
Na_2CO_3	0.12
Na_2SO_4	0.22
Na_3PO_4	0.018
NaCl	1.57
NaF	0.26
NaI	0.021
$NaNO_2$	11.9
$NaNO_3$	1.28
NaOH	1.44
Nd_2O_3	0.56
$Ni(OH)_2$	2.35
$PbSO_4$	0.39
SiO_2	2.23
$SrCO_3$	0.098
Zeolite	1.59
ZnO	0.22
ZrO_2	1.00
Insoluble Solids	12.8
Soluble Solids	3.04
Total	15.4

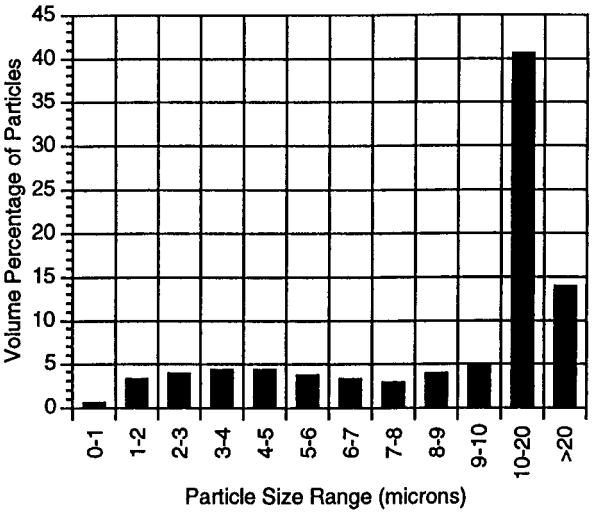

FIGURE 3. Particle size distribution for Purex simulated sludge.

TABLE 4. OPERATIONAL PARAMETER MATRIX

Test Number	Axial Velocity (ft/s)	Feed Pressure (psi)
1	6	30
2	8	40
3	2	30
4	6	15
5	8	20
6	6	30
7	4	40
8	6	45
9	10	30
10	4	20
11	6	30

used by JMP® software to produce a model to predict the filtrate flow rate under a variety of conditions, and a confidence interval for this prediction.

THEORY

The primary objective of this work was to develop a correlation for facility performance based on bench-scale testing. Ideally, this correlation would be developed on the basis of a theoretical understanding of the filtration process. It has been observed that cross-flow filtration can be divided into two regimes.[3] At low transmembrane pressures and high axial velocities, filtrate flux is generally linearly dependent on the radial pressure drop across the filter. However, at high operating pressure differences, filtrate flux is frequently independent of pressure drop due to the limitation of back transport of material from the surface of the filter.

The flux through the filter (J) can be described as:[4]

$$J = \frac{\Delta P}{\mu(R_F + R_c)} \tag{1}$$

where ΔP is the pressure drop across the filter, μ is the viscosity of the filtrate, R_F is the resistance of the filter, and R_c is the resistance of the filter cake. At low pressures, R_c does not vary with pressure (or is small) and filtrate flux is linearly dependent on the pressure drop across the filter. Under these conditions, the filter cake is not well developed and the resistance of the filter dominates the filtration performance. This filtration envelope will be referred to as pressure-dominated filtration throughout this report. As pressure increases, a cake develops on the surface of the filter and R_c becomes large and varies with pressure, typically linearly such that filtrate flux is then independent of pressure. Under these conditions, increases in axial velocity tend to produce decreases in R_c and thus increases in filtrate flux, while changes in pressure generally do not result in significant changes in filtrate flux. This filtration operational envelope will be referred to as axial velocity-dominated filtration. Under these conditions, a number of different models have been proposed to predict the filtrate flux.

A limited number of models have been developed to describe the dependence of R_c on operational parameters. These models tend to be empirical and fail to describe a number of significant phenomena that are observed during filtration. A second group of models has been more fully developed from back transport considerations and predict that the filtrate flux will be a function of shear rate and particle size but not an explicit function of pressure. Furthermore,

these models generally assume that the fluid flow is laminar in nature. Zydney and Colton have performed an in-depth review of these models.[5] These models have the generic form of

$$J \propto \frac{\gamma_w^{\alpha} D_p^{\beta}}{\nu^{\gamma}} \qquad (2)$$

where γ_w is the shear rate at the filter surface, ν is the kinematic viscosity of the slurry, and D_p is the particle diameter. Values for α have been reported between 0.33 and 3, β between -0.66 and 3, and γ between 0 and 1.[6,7,8] Gaddis has proposed a model that provides filtrate flux dependency on both axial velocity and pressure drop.[9] However, that model is limited to diffusion back transport and is thus of limited utility for systems involving large (micron-sized) solute particles. The dependencies predicted by Equation 2 will be compared to experimental data obtained from tetraphenylborate slurries.

RESULTS

As indicated in Tables 2 and 4, filtrate fluxes were obtained under a wide variety of conditions. In excess of 100 data points were collected during this experimental effort. The first step in understanding the filtrate flux for these slurries is generally to perform a pressure scan of filtration operation to identify the stage of development of the filter cake. This determination can be accomplished by inspecting the dependence of the average filtrate flux for each 30-minute time interval on pressure drop at a given axial velocity (6 ft/s). Note that a decline in filtrate flux was observed over this time period. However, the goal of this work is to provide a prediction for facility performance, and facility backpulse frequency is expected to take place as frequently as every 30 minutes. Thus, this prediction must employ an analysis of filtrate flows based on the average production over the backpulse period. Inspection of this segment of the data (see Figure 4) indicates that filtrate flux is not independent of pressure drop. Note that the usual interpretation of this occurrence is that a filter cake has not developed on the surface of the filter. However, further inspection indicates that filtrate flux is not linearly dependent on pressure drop as expected if no filter cake exists. Furthermore, filtrate flux was observed to vary with changes in axial velocity, indicating a significant filter cake was forming.

Thus, the system appears to be in transition from the regime of pressure-dominated filtration to axial velocity-dominated filtration. The

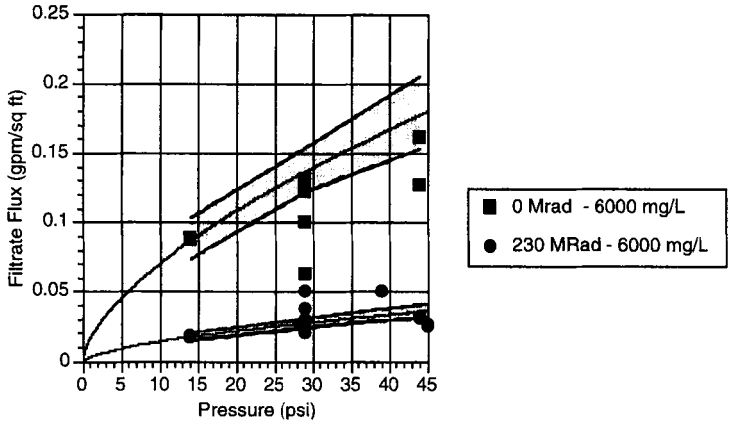

FIGURE 4. Filtrate flux as a function of pressure drop across the filter. Shaded areas are 95% confidence intervals for the prediction.

models outlined in the previous section will not provide reliable predictions of the filtrate flux since these models do not explicitly call out a dependency of filtrate flux on pressure difference. Furthermore, while the regime of operation represents a significant operational span for production facilities, little or no theoretical development has been completed for this operating envelope. Thus, an empirical predictive model was developed, based loosely on these previous models.

This new model will be of the form

$$J = C_1 f(d) V^{C_2} \Delta P^{C_3} e^{C_4 I} \tag{3}$$

where C_i are empirical constants, V is the axial velocity rather than the shear rate, I is the concentration of insoluble sludge solids, and f(d) is a function of the irradiation dose.

While the presence of insoluble sludge solids produces a measurable decrease in filtration performance, a theoretical dependency of the filtration performance on the concentration of insoluble sludge solids is not currently available, and thus this empirical form was selected.

Note that particle size and viscosity are changed through the irradiation process. Particle size analysis indicates that irradiation to 90

Mrad produces a decrease in average particle diameter from 2.7 to 2.1 microns (see Figure 5) and causes the slurry viscosity to decrease from 26 to 3 cp.[10] However, further irradiation does not produce further measurable decreases in particle diameter or produce any further measurable decrease in viscosity. Equation 2 indicates that many theoretical developments predict the filtrate flow rate to be a function of both slurry viscosity and particle size. However, since particle size and viscosity vary concomitantly upon irradiation, it was not possible to separate the influence of changes in these variables on filtrate flow. Furthermore, irradiation produces a significant number of organic degradation products (such as phenol, bi-phenyl, and phenyl boric acid) as well as producing changes to the surface chemistry of the slurry particles. Thus, while it is recognized that the irradiated and unirradiated slurries represent dramatically different slurries, it is insightful to explore if these two different fluids exhibit the same tendencies during the filtration process.

Analysis of the data using the JMP® statistical software provided the following expression for the filtrate flux, in gpm/ft^2:

$$J = 0.0137\ f(d)\ V^{0.355}\ \Delta P^{0.619}\ e^{-8.5\times10^{-5}\ I} \qquad (4)$$

where f(d) is 1 for a dose of 0 Mrad and is 0.20 for 90 Mrad or greater.

The dependence of filtrate flux on axial velocity is shown by plotting filtrate flux as a function of axial velocity (see Figure 6) at constant pressure (29 psi), constant insoluble sludge solids concentration (6000 mg/L), and two irradiation levels (0 and 230 Mrad). The prediction from Equation 4 is represented by the shaded areas on the plot. Note that only a limited segment of the data is presented in this plot for simplification since a plot of the complete data set produces a complex three-dimensional plot wherein it is not possible to indicate the confidence interval. Also note that all of the data generated during these experiments were employed in developing this model. The center line in these shaded areas represents Equation 4.

However, there is significant scatter in the experimental data, and thus there is a certain amount of uncertainty associated with this prediction. The shaded area represents the 95% confidence interval for this prediction. Note that this interval does not represent a 95% confidence interval for each data point. Thus, while any given data point may fall outside of the confidence interval, one can be 95% confident that the average filtrate flow rate will fall within the shaded interval. When an average filtrate flux is measured during facility tests, this value can then be employed with

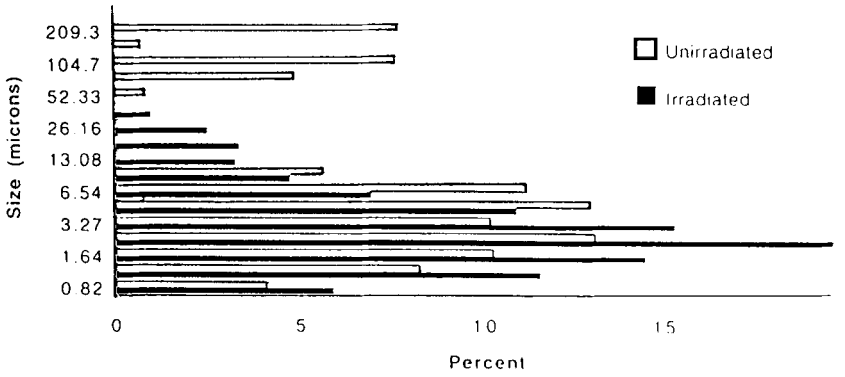

FIGURE 5. Particle size distribution for irradiated and unirradiated tetraphenylborate slurries.

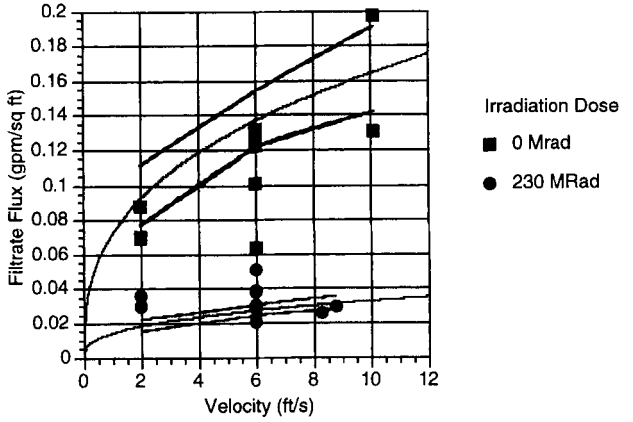

FIGURE 6. Filtrate flux as a function of axial velocity. Shaded areas are 95% confidence intervals for the prediction.

Equation 4 to predict the average filter performance with irradiated material. In addition, the data presented in this figure (and all subsequent figures) is only a subset of the complete data set, and thus, while trends may be difficult to discern from the limited data presented, analysis of the entire data set is employed in determining both the average and the 95% confidence interval. These 95% confidence intervals can also be interpreted as representing the impact of a given variable on filter performance. For example, if the upper value of the 95% confidence interval at low axial velocity were greater than the lower value of the 95% confidence interval at high axial velocity, the impact of velocity on filter performance would be statistically insignificant. However, this is not the case, indicating that velocity does play a statistically significant role in determining filtrate flux. This analysis has been performed on all of the variables employed in Equation 4. All of these variables were found to be statistically significant. In addition, cross terms were investigated to determine if any of the variables either increased or decreased the importance of the other variables. No statistically significant cross effects were found.

Inspection of Figure 6 and Equation 4 indicates the dependence of filtrate flux on axial velocity. However, shear rate at the surface of the wall was not measured during these tests since a transition exists within the data set from laminar to turbulent flow ($Re < 2000$ for unirradiated slurries, $2\,900 < Re < 14{,}000$ for irradiated slurries over the range of axial velocities). For turbulent flow, the shear at the wall has been related to the square of the velocity.[9] Thus, given these limitations, axial velocity was employed in this model in place of the shear rate at the surface of the filter (as in Equation 2).

Additional analysis was performed to determine if irradiation beyond 90 Mrad produced a statistically significant impact on filtrate flux. This analysis indicated that a slight dependence may exist. However, this dependence was significantly smaller than the dependence on any of the other variables included in Eqn. 4 and was found to be only marginally statistically significant. A comparison of Eqn. 4 ($f(d) = 1$ for 0 Mrad, $f(d) = 0.2$ for > 90 Mrad), and a modification of Eqn. 4 (that employed three values for $f(d) = 1$ for 0 Mrad, $f(d) = 0.18$ for 90 Mrad, and $f(d) = 0.22$ for 230 Mrad) is shown in Figure 7 at constant pressure (29 psi) and constant sludge solid concentration (6000 mg/L). Inspection of this figure indicates that there is not a significant difference between the dependence on irradiation predicted by separate consideration of the impact of 90-Mrad and 230-Mrad irradiation levels on filter performance.

The third parameter in Eqn. 4 is the applied pressure across the filter (transmembrane pressure). A plot of the filtrate flux as a function of

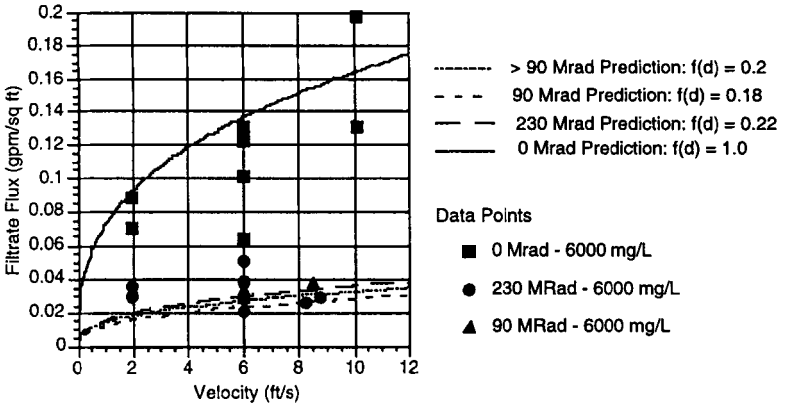

FIGURE 7. Filtrate flux predictions using average value for f(d) or two values for f(d).

pressure at constant axial velocity (6 ft/s), insoluble sludge solids concentration (6000 mg/L), and at two irradiation levels (0 and 230 Mrad) is presented in Figure 4. This figure indicates that the filtrate flux increases as the pressure increases. However, this increase is not linear with pressure drop. This type of dependence of filtrate flow indicates that the filtrate flux is only partially limited by filter cake development. This result indicates that over the 0 to 40 psig pressure range this filtration system is in transition from pressure-controlled filtration (where C_3 is 1) to axial velocity-controlled filtration (where C_3 is 0).

As part of the experimental design, the importance of the presence of insoluble sludge solids in the feed slurry was also investigated. The influence of 6000 mg/L sludge on filtrate flux can be observed by inspection of Figure 8. The data presented in this figure represent the filtrate fluxes obtained with and without the presence of sludge for slurries exposed to 0 and 230 Mrad of irradiation. Both data sets indicate that there is a significant (35%) decrease in filtrate production due to the presence of sludge. At the present time, there is not a clear theoretical understanding of the impact of insoluble sludge solids on filter performance. Bixler and Rappe also noted that the introduction of solid particulates into the feed slurry produced significant changes in filtrate fluxes.[11] However, while sludge plays a significant role in determining the final filtrate flux, the statistical analysis indicated that the presence of sludge did not change the trends observed for pressure, velocity, or irradiation.

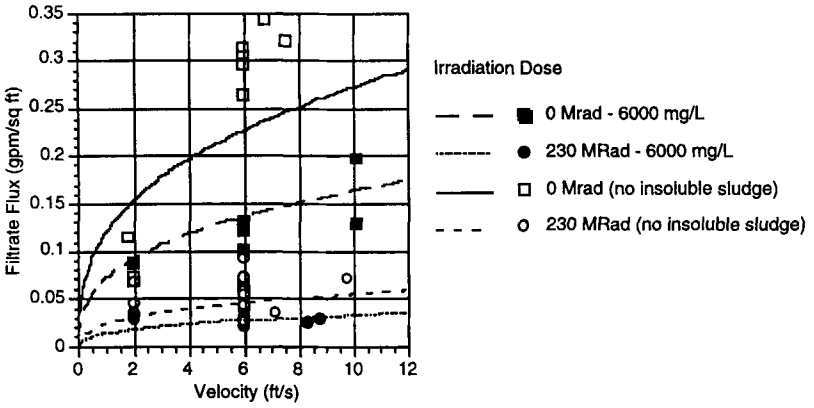

FIGURE 8. Filtrate flux as a function of insolubles content.

CONCLUSIONS

Due to the complexity of the changes that occur upon irradiation and the addition of sludge solids, this data set could not be used to develop an explicit understanding of the transport mechanisms involved in this filtration process. However, exposure to irradiation and the addition of sludge solids were both found to significantly decrease the filtrate flux. Furthermore, these tests indicate a significant gap exists in the theoretical understanding of filter performance that is of vital interest to production facilities.

A large body of experimental data on the filtration of tetraphenylborate slurries was collected. These data indicated that the filtrate flux was dependent on axial velocity and pressure drop. This dependency on both variables is not predicted by various theoretical interpretations. These trends would indicate that this filtration process occupies the region of filter operation over which filter cake is developing. An empirical model was developed to allow for the prediction of facility performance on the basis of lab-scale tests.

Additional tests with simplified systems to examine this operational envelope involving the development of filter cake would help illuminate this area of interest.

BIBLIOGRAPHY

[1] J.R. Fowler, J.T. Carter, L.F. Landon, J.C. Marek, C.L. Pearson, and S.M. Peters, Development of Feed Simulant Specifications for Integrated Cold Runs in the Defense Waste Processing Facility (U), Report WSRC-RP-89-238 Rev. 1, November 1, 1990.
[2] J.P. Bibler, Particle Size Analysis, Report SRT-LWP-94-132, December 27, 1994.
[3] M. C. Porter, Ind. Eng. Chem. Prod. Res. Develop. *11*, No. 3, (1972).
[4] G. Foley, P.F. MacLoughlin, and D. M. Malone, Sep. Sci. Tech. *30(3)* , 383, (1995).
[5] A. L. Zydney and C. K. Colton, Chem. Eng. Commun. *47*, 1, (1986).
[6] Ho,B.P., and Leal, L.G., J. Fluid Mech. *65*, 365 (1974).
[7] Vasseur, P., and Cox, R.G., J. Fluid Mech. *78*, 385 (1974).
[8] Zawicki, I., Malchesky, P.S., Smith, J.W., Harasaki, H., Asanuma, Y., and Nose, Y., Artificial Organs *27*, 539 (1981).
[9] J.L. Gaddis, Chem. Eng. Comm. *116*, 153, (1992).
[10] P.R. Monson, Westinghouse Savannah River Company, Aiken, South Carolina, unpublished data, 1994.
[11] Bixler, H.J., Rappe, G.C., U.S. Patent 3,541,006 (1970).